

## Boson-Fermion coherence in a spherically symmetric harmonic trap

Takahiko Miyakawa and Pierre Meystre

Optical Sciences Center, The University of Arizona, Tucson, AZ 85721

(Dated: March 23, 2002)

We consider the photoassociation of a low-density gas of quantum-degenerate trapped fermionic atoms into bosonic molecules in a spherically symmetric harmonic potential. For a dilute system and the photoassociation coupling energy small compared to the level separation of the trap, only those fermions in the single shell with Fermi energy are coupled to the bosonic molecular field. Introducing a collective pseudo-spin operator formalism we show that this system can then be mapped onto the Tavis-Cummings Hamiltonian of quantum optics, with an additional pairing interaction. By exact diagonalization of the Hamiltonian, we examine the ground state and low excitations of the Bose-Fermi system, and study the dynamics of the coherent coupling between atoms and molecules. In a semiclassical description of the system, the pairing interaction between fermions is shown to result in a self-trapping transition in the photoassociation, with a sudden suppression of the coherent oscillations between atoms and molecules. We also show that the full quantum dynamics of the system is dominated by quantum fluctuations in the vicinity of the self-trapping solution.

PACS numbers: 03.75.Lm, 03.75.Ss, 42.50.Ar

## I. INTRODUCTION

The formation of ultracold diatomic molecules from Feshbach resonances and photoassociation has witnessed spectacular developments in recent years. Early demonstrations of molecule formation using two-photon Raman photoassociation [1] and a Feshbach resonance [2] were dominated by the molecular losses due to processes such as inelastic decay to lower energy molecular vibrational states [3], so that the existence of the molecules could only be inferred from the decrease in the number of atoms. The first unambiguous coherent conversion of atoms into molecules was performed by Donley et al. [4], who exploited a Feshbach resonance in a  $^{85}\text{Rb}$  Bose-Einstein Condensate (BEC). In subsequent experiments starting from an atomic condensate of  $^{87}\text{Rb}$ , Rempe and coworkers used adiabatic rapid passage to create the molecules [5]. Because the molecules and atoms have different magnetic moments, they could be spatially separated from each other using a magnetic field gradient via the Stern-Gerlach effect. Similar work has been conducted by Xu et al. [6]. Starting from a sodium BEC, they used resonant laser light to blast away the remaining atoms in the sample and isolated the molecules. Unfortunately, the conversion efficiency was limited by inelastic losses very close to the resonance so that molecular yields were  $< 10\%$ .

For fermionic atoms close to a Feshbach resonance the inelastic collision rate for relaxation to lower energy vibrational states of the molecules scales like  $a(B)^{2.55}$  whereas for bosons it scales like  $a(B)$  where  $a(B)$  is the scattering length near the resonance [7]. This is because close to resonance the effective size of the molecules is of the order  $a(B)$ , which is comparable to the interparticle spacing. In order for a molecule to decay to a more deeply bound vibrational state with radius  $R_e$   $a(B)$ , the atoms comprising the molecule along with an additional atom must all collide within a distance  $R_e$ .

Since two of the three atoms are necessarily identical, the collision rate is suppressed for fermions. Taking advantage of this consequence of the Pauli Exclusion Principle, Greiner et al. [8] achieved the first molecular BEC by starting from a quantum degenerate spin mixture of  $^{40}\text{K}$  using adiabatic rapid passage through a Feshbach resonance with a conversion efficiency of  $\sim 80\%$ . At about the same time Zwierlein et al. [9] and Jochim et al. [10] succeeded in producing a BEC of  $^6\text{Li}_2$  dimers by evaporatively cooling the atoms at a constant magnetic field just below a resonance where  $a(B)$  is large and positive. Two recent experiments have led to the observation of heteronuclear Feshbach resonances in Bose-Fermi mixtures of  $^6\text{Li}$  and  $^{23}\text{Na}$  [11] in one case, and of  $^{87}\text{Rb}$  and  $^{40}\text{K}$  in the other [12]. We also mention recent experiments by Kerman et al. [13], who produced metastable  $\text{RbCs}$  molecules in their lowest triplet state starting from a laser-cooled mixture of  $^{85}\text{Rb}$  and  $^{133}\text{Cs}$  by photoassociation. Major current experimental and experimental efforts are directed towards the exploration of the crossover between the Bardeen-Cooper-Schrieffer (BCS) state of fermionic atoms and BEC of bosonic molecules as the system crosses a Feshbach resonance [14]. In the vicinity of these resonances, the system enters a strongly interacting regime that offers a challenge for many-body theories [15, 16].

It is known that the pairing properties of finite-size systems can be significantly different from those of the bulk material, due to the discrete energy spectrum of the particles involved. The detailed role of the shell structure has been explored both in the nuclei [17] and of superconductor grains [18], in which a collective character of pairs plays an important role. In this paper we consider the photoassociation of a dilute quantum-degenerate gas of fermionic atoms trapped in a spherically symmetric harmonic trap into molecular dimers, including the pairing interaction between fermions. By introducing a pseudo-spin formalism for the time rever-

pairing operator [19, 20], this problem can be mapped onto an extension of the Tavis-Cummings model [21, 22] that describes the coupling of  $N$  two-level atoms and a single mode of the electromagnetic field, and has found applications in the study of superradiance in quantum optics [23, 24]. This analogy allows us to study in detail the ground state and lower excited states of the system, as well as the coherent dynamics of atom-molecule coupling in the trap. We show that for appropriate conditions, only those fermions on the last energy shell of the trap participate in the photoassociation process, and discuss the impact of the filling of that shell on molecule formation. We find that depending on the detuning of the photoassociation laser from the energy difference between the molecules and atom pairs, the nature of the ground state changes from being predominantly atomic to predominantly molecular in nature. We study the crossover between these two regions in detail, and quantify its property via the joint coherence of the atomic and molecular fields and the entanglement entropy of the system.

The coherent conversion of fermions into bosons has been studied in the homogeneous case by several authors [15, 25, 26]. Trapped systems, in addition to being closer to the experimental situation, present several unique characteristics: First, the discreteness of the energy levels eliminates many of the difficulties associated with a continuum. In addition, the high degeneracy of spherically symmetric harmonic potentials simplifies significantly the study of coherent quantum dynamics. Indeed, the problem resembles then the dynamics of a bosonic Josephson Junction [27, 28], although the nonlinear coupling between fermionic atoms and bosonic molecules leads to considerably richer dynamics. Moreover the additional pairing interaction between fermions is shown to result in a self-trapping transition [27, 29], with a sudden suppression of the coherent oscillations.

This paper is organized as follows. Section II discusses our model and formulates it in terms of a pseudo-spin formalism. Section III presents results of the static problem where the many-body states are classified by number of unpaired fermions known as seniority [30] in nuclear physics. We show that for a fixed number of atoms, the ground state of the system is always the state of minimum seniority. We examine the crossover behavior of the ground state as the detuning parameter is varied, as a function of the ratio of the total number of fermionic pairs and molecules to the degenerate number of the Fermi level. The entanglement between fermions and bosons is evaluated and found to be reduced as the pairing interaction becomes stronger. In section IV, we analyze the coherent dynamics of the nonlinear atom-molecule coupling. Using a semiclassical factorization ansatz, we show the appearance of a self-trapping transition in the presence of pairing interaction. An exact quantum solution shows that around that transition point the dynamics is characterized by large quantum fluctuations. Finally, section V is a summary and outlook. Computational details are relegated to an appendix.

## II. MODEL

We consider a trapped dilute gas of two-component fermionic atoms in hyperfine states of spin  $= \uparrow, \downarrow$  at zero temperature and coupled to a single mode gas of bosonic molecules via a two-photon Raman transition. The trap is assumed to be harmonic and spherically symmetric, described by the potential

$$V_f = \frac{1}{2} m_f \omega_{ho}^2 r^2 \quad (1)$$

for the atoms, and similarly with  $m_b$  for the bosonic molecules.

In the absence of interactions between particles, the trap levels have the energies

$$E_n = \left(n + \frac{3}{2}\right) \hbar \omega_{ho} \quad (2)$$

where the principal quantum number  $n$  is positive or zero. In order to deal with the high degree of degeneracy of this potential, it is convenient to introduce the (integer) radial and angular quantum numbers  $n_r$  and  $l$ , which are positive or zero, with [31]

$$n = 2n_r + l \quad (3)$$

Each pair  $(n_r; l)$  corresponds to a radial wave function  $R_{n_r, l}(r)$  and hence  $(2l + 1)$  common eigenfunctions of  $V_f(r)$ ,  $L^2$  and  $L_z$ ,

$$\psi_{n_r, l, m}(r) = R_{n_r, l}(r) Y_{lm}(\theta, \phi) \quad (4)$$

Taking into account the magnetic quantum number

$$l = m + l; \quad (5)$$

the degeneracy of each level  $E_n$  is therefore

$$g_n = \frac{1}{2} (n + 1)(n + 2); \quad (6)$$

and the total number of states up to the shell  $n_F$  corresponding to the Fermi energy

$$E_F = \left(n_F + \frac{3}{2}\right) \hbar \omega_{ho}$$

is

$$N_{n_F} = 2 \sum_{n=0}^{n_F} g_n = \frac{1}{3} (n_F + 1)(n_F + 2)(n_F + 3);$$

where the factor of 2 accounts for the two hyperfine spin states of the atoms. In the following, it will be necessary to include the attractive interaction responsible for the pairing between fermions. Since as we show later on this interaction splits the degeneracy of the trap levels, we keep the angular momentum index in the labelling of the atomic energies,  $E_{n_r, l}$ . The fermionic atoms are therefore

described by the annihilation operator  $c_{n,l,m}$ , where  $n$  labels the hyperfine spin state of the atom with single-particle wave function  $\psi_{n,l,m}(\mathbf{r})$  and eigenenergy  $E_{n,l}$ .

Assuming that the atom-molecule photoassociation energy is smaller than the trap energy spacing,  $\hbar\omega_{ho}$ , and in addition that the system is sufficiently dilute that the attractive interaction between fermions is likewise less than  $\hbar\omega_{ho}$ , it is possible to tune the frequency of the photoassociation laser so as to only couple fermions in the shell  $n_F$  with Fermi energy  $E_F$  to molecules in the ground state of the harmonic trap. We can then ignore all shells other than the  $n_F$ -shell for the fermions, and all trap states above the ground state for the molecules, which are then described in terms of the ground state bosonic annihilation operator  $b$  with single particle energy  $E_0$ .

Both atomic pairing and photoassociation involve the creation and annihilation of pairs of atoms, hence it is convenient to introduce pseudo-spin operators  $S_l$  [20] for atoms of angular momentum  $l$  in the  $n_F$ -shell as

$$S_l^+ = \sum_{m=-l}^l (-1)^{l-m} c_{l,m}^\dagger c_{l,-m}^\dagger; \quad (7)$$

$$S_l = \sum_{m=-l}^l (-1)^{l-m} c_{l,m} c_{l,-m}; \quad (8)$$

$$S_l^z = \frac{1}{2} \sum_{m=-l}^l c_{l,m}^\dagger c_{l,m} = \frac{1}{2} (\hat{n}_l - 1); \quad (9)$$

where  $1 = 2l+1$  and  $\hat{n}_l$  is number operator in each level  $l$ . (Here and hereafter we have omitted the label  $n_F$  from the fermionic operator  $c_{n_F,l,m}$ .) They are easily seen to obey the SU(2) algebra

$$[S_l^+, S_l^z] = 2S_l^z; \quad [S_l^z, S_l^z] = 0; \quad (10)$$

Since we need only consider atoms in the Fermi level, the total number of relevant particles in the system is

$$N = n_p + n_b + M; \quad (11)$$

where

$$M = n_p + n_b \quad (12)$$

is the number of molecules ( $n_b$ ) and atomic pairs ( $n_p$ ) in the  $n_F$ -shell, or loosely speaking the number of pairs, and  $1$  is the number of unpaired atoms in the  $n_F$ -shell. In that reduced Hilbert space, a complete set of states is given by

$$|j_1; n_1^0; j_0; n_0; i\rangle = \frac{1}{N} (S_l^+)^{n_1} (S_l^z)^{n_1^0} (S_l^z)^{n_0} (b^\dagger)^{n_b} |i\rangle; \quad (13)$$

where  $N$  is a normalization constant.

For a given angular momentum  $l$ , the possible number of atomic pairs  $n_1$  in the Fermi level is

$$0 \leq n_1 \leq 1 = 2l+1;$$

while the number of molecules is  $0 \leq n_b \leq N$ .

The pseudo-spin operator  $S_l$  annihilates atoms in pairs, hence any state  $|j_1; j_0; j_0^0\rangle$  of unpaired fermions and zero molecules clearly satisfies

$$S_l |j_1; j_0; j_0^0\rangle = 0; \quad \hat{n}_b |j_1; j_0; j_0^0\rangle = 0; \quad (14)$$

with

$$\hat{n}_l |j_1; j_0; j_0^0\rangle = j_1 |j_1; j_0; j_0^0\rangle; \quad (15)$$

see Eq. (11). The number operator of bosonic molecules has been defined by  $\hat{n}_b = b^\dagger b$ .  $1$  is the number of unpaired fermions of angular momentum  $l$  in each level and is referred to as seniority [30] in nuclear physics.

With this formal development at hand, we now turn to the discussion of the fermionic pairing and of the photoassociation of atoms into molecules. It is described by the effective Hamiltonian

$$H = (\hbar\omega_{ho} + E_0) b^\dagger b + \sum_{l,m} E_{n_F,l} c_{l,m}^\dagger c_{l,m} + V_p + V_{am}; \quad (16)$$

where  $\omega_{ho}$  is the two-photon detuning between the Raman lasers and the internal energy difference between atomic pairs and molecules,  $V_p$  describes atomic pairing and  $V_{am}$  accounts for the photoassociation of atoms into molecules. Before discussing these two interaction Hamiltonians in detail, we first evaluate the mean-field lifting of the single-particle energy degeneracy,  $E_{n_F} = E_{n_F,l}$ .

In the s-wave scattering approximation, valid at  $T = 0$ , atoms of opposite spin interact via the two-body interaction potential

$$V(\mathbf{r}_1 - \mathbf{r}_2) = \frac{4\hbar^2 a}{m_f} \delta(\mathbf{r}_1 - \mathbf{r}_2); \quad (17)$$

where  $a < 0$  is the scattering length, negative for attractive interactions. In the Thomas-Fermi limit, this results in the atoms being subjected to the mean-field potential

$$V(\mathbf{r}) = \frac{2\hbar^2 a}{m_f} \rho(\mathbf{r}); \quad (18)$$

where the density  $\rho(\mathbf{r})$  is given by

$$\rho(\mathbf{r}) = \frac{1}{4} (1 - r^2/R_{TF}^2)^{3/2}; \quad (19)$$

for

$$r \leq R_{TF} = a_{ho} \sqrt{2n_F + 3}$$

and is zero otherwise. Here  $a_{ho} = \hbar/m_f \omega_{ho}$  is the oscillator length and  $\omega_{ho} = (2n_F + 3)^{3/2} \omega_{ho}^0$ . The resulting mean-field energy splitting of the  $l$ -states within the  $n_F$  manifold is then [32]

$$E_{n_F,l} = \frac{E_{n_F}}{Z_{n_F}} = \int d\mathbf{r} r^2 V(\mathbf{r}) \mathcal{R}_{n_F,l}^2 \quad (20)$$

$$= \frac{2}{3} \frac{a}{a_{ho}} (2n_F + 3)^{3/2} \hbar\omega_{ho}^0 \frac{4}{3} \frac{1}{4} \frac{l(l+1)}{n_F^2};$$

where we have used the WKB limit of the radial harmonic oscillator wave function which is valid for  $n_F \gg 1$ . For an atomic system to be dilute, the mean-field shift Eq. (20) should be less than the unperturbed energy  $E_n$ . This implies that

$$n_F^{1/2} \frac{\hbar^2 j}{a_{ho}} \ll 1; \quad (21)$$

which is equivalent to the familiar diluteness condition  $\rho \hbar^3 \ll 1$ .

It is known that for attractive short range interactions, the potential  $V(r_1 - r_2)$  favors the creation of a time-reversal state and lets pairing take place. The Hamiltonian  $V_p$  describes this pairing correlation by including only the correlations for time-reversal pair states

$$J = 0; M = 0; l_1 l_2 = \begin{matrix} X^1 \\ (l_1; l_2 = j_0) j; m_1 j; m_2 \\ m = 1 \end{matrix} \quad (22)$$

where

$$(l_1; l_2 = j_0) = (-1)^m (2l_1 + 1)^{-1/2} \quad (23)$$

is a Clebsch-Gordan coefficient. Assuming for simplicity that the radial part  $g$  of the pairing interaction is independent of the angular momenta  $l_1$  and  $l_2$  of the atomic pairs involved in the interaction,  $V_p$  reads explicitly

$$V_p = \sum_{l_1 m_1} \sum_{l_2 m_2} (-1)^{l_1 + l_2} \sum_{m_1 m_2} C_{l_1 m_1}^Y C_{l_2 m_2}^Y C_{l_1 m_1}^0 C_{l_2 m_2}^0; \quad (24)$$

where the terms  $(-1)^{l_1 + l_2}$  and  $(-1)^{m_1 + m_2}$  come from the Clebsch-Gordan coefficients (23) and hence account for the angular part of the wave functions. Strictly speaking, the coupling constant  $g_{l_1 l_2}$  should be determined by the spatial integral

$$g_{l_1 l_2} = \frac{4 \hbar^2 \hbar^2 j}{m_f} \int dr r^2 R_{n_F, l_1}^2(r) R_{n_F, l_2}^2(r); \quad (25)$$

However for our present purpose it is sufficient to estimate  $g$  by replacing the spatial integral in Eq. (25) by  $\hbar^2 n_F^{-3/2}$ , where for a pure harmonic oscillator state in the  $n_F$ -shell the mean square radius  $\hbar^2 n_F^{-3/2}$  is given by  $(2n_F + 3)a_{ho}^2$  from the virial theorem. This gives

$$g = \frac{4 \hbar^2 \hbar^2 j}{m_f} (2n_F + 3)^{-3/2} a_{ho}^{-3} \frac{\hbar^2 j}{a_{ho}} n_F^{-3/2} \hbar^2 n_{ho}; \quad (26)$$

In this model, the strongest pairing occurs for degenerate energies,  $E_l = E_{l^0}$  for all  $l; l^0$ . We will see that all fermions in the  $n_F$ -shell are then coherently paired, the pairing energy being proportional to the degeneracy factor  $n_F$ . In the dilute gas limit, which is equivalent to  $g n_F \ll g_F^2 \hbar^2 n_{ho}$ , the pairing takes then place on a single shell, see Ref. [32] for more details.

Turning finally to the photoassociation of atomic pairs into molecules and the reverse process of photodissociation of molecules back into atoms, we note that it is

possible to neglect all processes involving atoms other than those in the  $n_F$ -shell provided that their characteristic frequency, the product  $\hbar \omega_{bi}$  of the photoassociation coupling constant,  $\gamma$ , and the square root of the mean number of molecules, remains small compared to the frequency separation between neighboring shells of the trap. This condition is well fulfilled for typical laser strengths and trap depths, in which case  $\hbar \omega_{bi} \sim 10^2 n_F^{-1/2} s^{-1}$ ,  $\hbar \omega_{ho} \sim 10^3 s^{-1}$ . In this case, the atom-molecule coupling can be approximated by the Hamiltonian

$$V_{am} = \sum_{l, m} (-1)^{l+m} C_{l m}^Y C_{l m}^Y b^\dagger + b^\dagger C_{l m}^Y C_{l m}^Y; \quad (27)$$

where we only include the coupling between time-reversal atomic pair and bosonic molecules in the ground state of the harmonic trap. The photoassociation coupling constant  $\gamma$  is proportional to the far off-resonant two-photon Rabi frequency associated with two nearly co-propagating lasers with frequencies  $\omega_1$  and  $\omega_2$  [1],

$$\gamma = \frac{\hbar}{4} \int dr r^2 R_{0,0}^{(b)}(r) R_{n_F, l}^2(r) \frac{\omega_1 \omega_2}{n_F a_{ho}^3}; \quad (28)$$

where  $R_{0,0}^{(b)}$  is a ground-state wave function of molecules of mass of  $2m_f$  with a spatial width about  $a_{ho}$ , and in the second equality we have again replaced the radial wave function of the atoms by  $\hbar^2 n_F^{-3/2}$ . From the coupling constant between  $^{87}\text{Rb}_2$  molecules and  $^{87}\text{Rb}$  atoms of Ref. [33] we estimate the photoassociation coupling constant to be of the order of  $\gamma = 7.6 \times 10^{-7} m^{-3/2} s^{-1}$ .

In terms of the pseudo-spin operators, and with Eqs. (24) and (27), the total model Hamiltonian Eq. (16) finally reads

$$H = (\hbar + E_0) b^\dagger b + 2E_{n_F, l} (S_1^Z + I_1 = 2) + \sum_{l, m} (S_1^+ b + b^\dagger S_1^-) g \sum_{l, l^0} S_1^+ S_{l^0}^-; \quad (29)$$

This Hamiltonian clearly conserves the spin operators  $S_1^2$ . Applying this operator on the state  $|j, i\rangle$  we have

$$\begin{aligned} S_1^2 |j, i\rangle &= S_1(S_1 + 1) |j, i\rangle \\ &= f S_1^+ S_1 + S_1^Z (S_1^Z - 1) g |j, i\rangle \\ &= (-I_1 = 2 - I_1 = 2) (-I_1 = 2 - I_1 = 2 + 1) |j, i\rangle; \end{aligned}$$

where we have used the identity  $S_1^2 = S_1^+ S_1 + S_1^Z (S_1^Z - 1)$  and Eqs. (14) and (15), so that

$$S_1 = \frac{1}{2} (-I_1 - I_1):$$

This allows us to identify the operator

$$\hat{M} = \sum_{l, m} (S_1^Z + S_1) + \hat{N}_b; \quad (30)$$

as the operator giving the total number of fermionic pairs and molecules, or loosely speaking the "pair number" operator, which is easily seen to also be a conserved quantity.

In the limit  $\delta \rightarrow 0$  the Hamiltonian (29) reduces to the Tavis-Cummings Model [21, 22] of quantum optics, while for  $\delta \neq 0$ , it becomes the Pairing Model [34, 35], for which Richardson first gave an exact solution in the context of nuclear physics. We also mention a recent family of exactly solvable models of atom-molecule proposed in Ref. [36].

The discussion of the following sections concentrates especially in that situation where the mean-field energy shift in single-particle energies is smaller than the photoassociation coupling. In this degenerate model, the single-particle energies of all atoms in the  $n_F$ -shell can then be taken to be equal,  $E_{n_F, j} = E_F$ , and the Hamiltonian (29) simplifies to

$$H = \hbar\omega (S^z + S) + \hbar\omega (S^+ b + b^\dagger S) - \hbar g S^+ S; \quad (31)$$

where we have introduced the total spin operator

$$S = \sum_{j=1}^N S_j; \quad (32)$$

$\omega = \omega_0 + (E_0 - 2E_F)/\hbar$ ,  $n_F = \sum_{j=1}^N n_{F,j}$ ,  $S = \sum_{j=1}^N S_j$ , so that the total spin is

$$S = \sum_{j=1}^N S_j = \frac{1}{2} (n_F); \quad (33)$$

In Eq. (31), we have neglected constant terms proportional to the conserved quantity  $M$ .

Assuming an oscillator length  $a_{ho} = 3.2 \times 10^{-6}$  m for the mass of  $^6\text{Li}$ ,  $a = 114$  nm for its scattering length, and  $\omega_{ho} = 1000 \text{ s}^{-1}$ , then  $n_F^{3/2} \sim 10^2 \text{ s}^{-1}$ . The validity of the degenerate model,  $E_{n_F, j} - E_{n_F, j'} < n_F$  requires  $n_F < 10$ , which corresponds to a total number of fermions  $N_{n_F} < 10^3$ .

### III. GROUND STATE

In this section, we discuss the dependence of the ground state of the model Hamiltonian (31) on the ratio of number of paired fermions and molecules,  $M = n_p + n_b$ ; to the degeneracy of the Fermi level (we drop the subscript  $n_F$  for notational clarity from now on). We identify qualitatively different types of ground states, a pair-dominated ground state and a molecular-dominated one, as a function of the parameter

$$\frac{\omega}{g}; \quad (34)$$

where  $\omega = \omega_0 + (E_0 - 2E_F)/\hbar$  is the photoassociation frequency detuning.

#### A. Pairing Model

For a total number of particles  $N = 2M + 1$ , which corresponds to the Fermi energy shell less than half-filled since there are two hyperfine atomic states involved, the seniority can take the values

$$= \begin{cases} 0; 2; 4; \dots; N & (N \text{ even}) \\ 1; 3; 5; \dots; N & (N \text{ odd}), \end{cases} \quad (35)$$

while for  $N \geq 2$ , corresponding to a shell more than half-filled, the permissible values of are

$$= \begin{cases} 0; 2; 4; \dots; 2 & N & (N \text{ even}) \\ 1; 3; 5; \dots; 2 & N & (N \text{ odd}). \end{cases} \quad (36)$$

The degenerate Pairing Model of Refs. [37, 38] is obtained by neglecting the photoassociation coupling,  $\omega = 0$ , in the Hamiltonian (31). In this case, the total energy is given as a function of seniority and the total number  $N$  of fermions by

$$E_{pm}(N; s) = -\frac{1}{4} N (N - 1) (2s + N + 2); \quad (37)$$

and it is minimized for  $s = 0$  or  $1$ .

For an even particle number, the ground state corresponds therefore to all pseudo-spins aligned,  $S = N/2$ ,

$$E_{pm}(N; s = 0) = -\frac{1}{4} N (N - 1) (2s + N + 2); \quad (38)$$

The first excited state corresponds to  $s = 2$  unpaired atoms, or  $S = N/2 - 1$ , and its energy is

$$E_{pm}(N; s = 2) - E_{pm}(N; s = 0) = g; \quad (39)$$

Thus, the energy needed to break up an atomic pair into two unpaired fermions is independent of the number of fermions in the  $n_F$ -shell. This energy is consistent to Bogoliubov quasi-particle energy based on BCS variational state except for corrections of relative order  $1/N$ .

#### B. Photoassociation

In the presence of photoassociation,  $\omega \neq 0$ , the eigenstates of the system consist of a coherent superposition of atoms and molecules. For fixed  $N$ , we can classify them by the total spin  $S = (N - 1)/2$ , each manifold consisting of  $(M + 1)$  eigenstates, where  $M = (N - 1)/2 = n_p + n_b$  is the total number of pairs.

For positive detuning,  $\omega > 0$ , the ground state is a pure fermionic state, i.e.,  $N = 2n_p + 1$ . On the other hand, for a large negative detuning energy,  $\omega < 0$ , and even particle number, the ground state is reached when all particles are molecules, corresponding to a zero seniority, or maximum spin state.

Figure 1 shows the energies  $E$  of a few seniority states relative to that of the state  $s = 0$  as a function of  $\omega/g$ . This example is for  $n_p = n_b = 1$  and

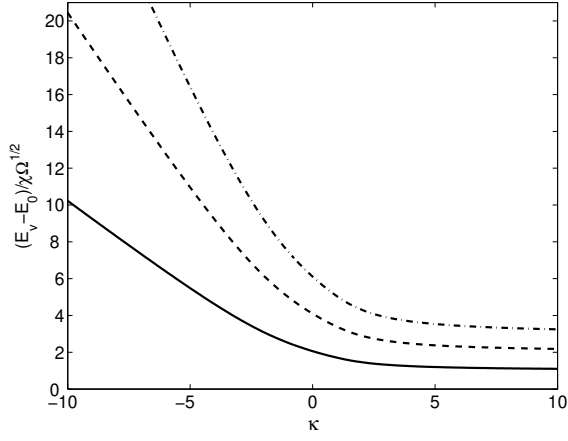


FIG. 1: Excitation energies, in units of  $\hbar \Omega^{1/2}$ , relative to the ground-state energy for the seniority states  $\nu = 2$  (solid line),  $\nu = 4$  (dashed line), and  $\nu = 6$  (dash-dotted line), as a function of the dimensionless parameter  $\kappa = \Delta / \hbar \Omega^{1/2}$  for  $g = 0$  and  $N = 120$ .

a half-filled Fermi energy shell,  $N = 120$ , corresponding to  $n_F = 14$ , and results from a direct numerical diagonalization of the Hamiltonian. It shows that over the wide range of  $\kappa$  considered here, the ground state is always the maximum spin manifold  $S = 0$ . For large negative detunings, the energy differences  $E - E_0$  are  $\approx 2$  times the single-particle energy difference between a molecule and two fermions, and increase with  $|j|$ . For large positive detunings, on the other hand, the energies of the excited states approach the values  $\approx 2$  times  $g$ , see Eq. (39). In the crossover region where the nature of the ground state changes from atomic to molecular, the ground state is a coherent superposition of atoms and molecules that is likewise the maximum spin state. We have verified that in the absence of pairing interaction,  $g = 0$ , the ground state is likewise the state of maximum spin (not shown in figure).

In the following we concentrate on the state of maximum total spin,  $S = 2i$ , for an even number of fermions,  $N = 2M$ . The eigenstates of the atom-molecule system in the spin manifold  $S = 2i$  have the general form

$$|j, S, i\rangle = \sum_{n_b=0}^M C(n_p) |S = 2i; S^z = S + n_p i_F\rangle_{n_b=0} \quad (40)$$

where  $n_p$  denotes a number of fermionic pairs and  $i_F = 0; 1; \dots; M$  represent eigenmodes of the system with eigenenergies  $E$ . We have found these eigenstates and the associated eigenenergies by direct diagonalization of the Hamiltonian (31).

The average number of molecules in the ground state is shown in Fig. 2 as a function of  $\kappa = \Delta / \hbar \Omega^{1/2}$  and  $M$  for  $g = 0$  and  $N = 120$ . As expected, for large positive

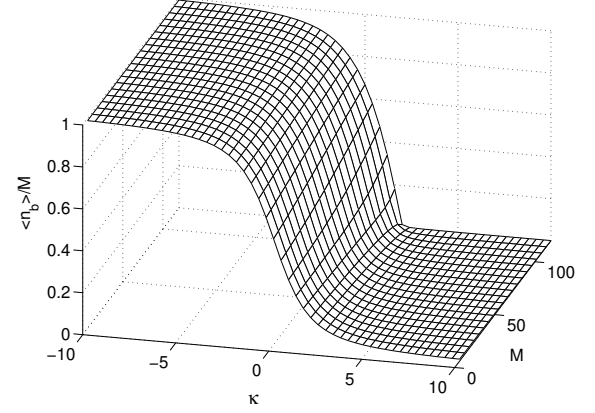


FIG. 2: Normalized average number of molecules in the ground state as a function of  $\kappa$  and  $M$  for  $N = 120$  and  $g = 0$ .

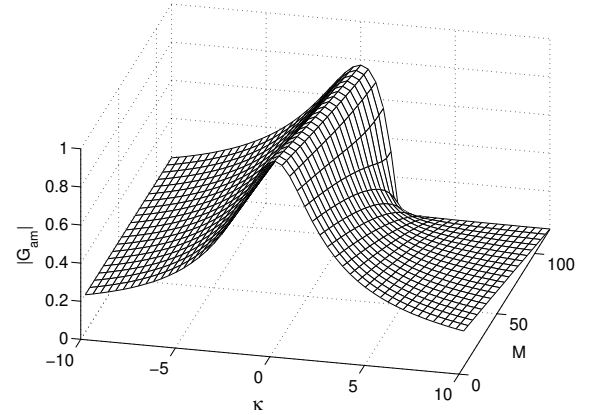


FIG. 3: Normalized joint coherence function,  $|G_{am}|$ , as functions of  $\kappa$  and  $M$  for  $N = 120$  and for  $g = 0$ .

detuning  $\Delta > 0$ , the ground state population consists almost exclusively of atoms, while it is mostly made up of molecules for large negative detunings. In the crossover region around  $\Delta = 0$ , the ground state consists of a coherent superposition state between molecules and atomic pairs.

It is possible to characterize this superposition in terms of the normalized joint coherence function

$$G_{am} = \frac{2\hbar S^+ b_i}{M}; \quad (41)$$

which is shown in Fig. 3 as a function of  $\kappa$  and the number of pairs  $M$ . The joint coherence of the atomic and molecular fields shows a remarkable enhancement in the crossover region as well as a change in shape as a function of  $M$ , due to the nonlinearity of the atom-molecule coupling (27). This dependence on the coupling factor  $M$  can be understood more quantitatively by considering the

two limiting cases  $M = 1$  and  $M = \infty$ .

### 1. $M = 1$ | Mapping on a linear coupled-boson system

In the limit of small coupling factors, it is convenient to describe the system in terms of the Holstein-Primakoff mapping [39] of the  $SU(2)$  generators  $S^+ = (S^x)^y$  and  $S^z$  in terms of bosonic operators. According to this mapping, the Hilbert space of the group  $SU(2)$  is carried by a subspace of the bosonic Fock space given by the bosonic vacuum  $|0\rangle_d$  and the bosonic operators  $d$  and  $d^\dagger$ , with

$$[d, d^\dagger] = 1; \quad d|0\rangle_d = 0; \quad (42)$$

The bosonic space being spanned by the  $n_d$  boson states

$$|n_d\rangle_d = \frac{1}{n_d!} (d^\dagger)^{n_d} |0\rangle_d \quad \text{for } n_d = 0, 1, 2, \dots, M :$$

Since we restrict our considerations to the subspace characterized by the angular momentum quantum number  $S = 1/2$ , we can map the operators  $S^+$  and  $S^z$  as

$$\begin{aligned} S^+ &\rightarrow \sqrt{1 - d^\dagger d} d^\dagger; \\ S^- &\rightarrow d \sqrt{1 - d^\dagger d}; \\ S^z &\rightarrow \frac{1}{2} + d^\dagger d; \end{aligned} \quad (43)$$

In the limit  $M = 1$ , we only need a lowest-order of the operators (43), that is, replace the square roots by 1. The Hamiltonian (31) reduces then to that of a linearly coupled two-mode boson system,

$$H \rightarrow H_{\text{linear}} = (\epsilon + g) d^\dagger d + \frac{1}{2} (d^\dagger b + b^\dagger d); \quad (44)$$

with the constraint  $M = n_d + n_b$ .

This Hamiltonian can be diagonalized by the transformation

$$\begin{aligned} c^- &= \cos \alpha d^- + \sin \alpha b^- \\ c_+^\dagger &= \sin \alpha d^\dagger + \cos \alpha b^\dagger; \end{aligned}$$

with  $\cot 2\alpha = (\epsilon + g)/2$ ,  $\alpha \in [0, \pi/2]$ , to give

$$H_{\text{linear}} = c_-^\dagger c_- + c_+^\dagger c_+; \quad (45)$$

with energies

$$\begin{aligned} E_- &= (\epsilon + g) \cos^2 \alpha - 2 \cos \alpha \sin \alpha; \\ E_+ &= (\epsilon + g) \sin^2 \alpha + 2 \cos \alpha \sin \alpha; \end{aligned}$$

Since  $\frac{1}{2} < \alpha$  for  $g > 0$ , the ground state is  $(1/M!) (c_-^\dagger)^M |0\rangle_d |0\rangle_b$ .

### 2. $M = \infty$ | Mapping on a binary atomic-molecular condensate

Tikhonenkov and Vardi [26] showed for in the homogeneous case that when the total number of pairs is equal to the available momentum states of the fermions, the system of fermionic atoms and bosonic molecules can be mapped onto a two-mode atomic-molecular BEC system [40, 41, 42]. The corresponding situation in our case occurs for  $M = 1$ , with an additional atom-molecule two-body collision term required in addition.

To show how this works we introduce the two-mode Hamiltonian of a two-component condensate of atoms and molecules,

$$H_{\text{am}} = \epsilon_a b_m^\dagger b_m + \frac{g}{2} (b_m^\dagger b_a b_a + \text{h.c.}) - \frac{g}{2} b_m^\dagger b_m b_a^\dagger b_a; \quad (46)$$

where  $b_a^\dagger$  and  $b_m^\dagger$  are the bosonic creation operators for the atomic and molecular modes, respectively. Clearly the total number of particles  $N_{\text{am}} = n_a + 2n_m$  is conserved, where  $n_a$  and  $n_m$  are the number of atoms and molecules, respectively. For  $N_{\text{am}}$  even, a general state of the system can be expressed as

$$\begin{aligned} |j_{\text{am}}\rangle &= \sum_{m_a=0}^{M/2} C(m_a) |j_a = 2m_a\rangle |j_m = M - m_a\rangle \\ &= \sum_{m_a=0}^{M/2} C(m_a) |2m_a; n_m\rangle; \end{aligned} \quad (47)$$

with  $M = N_{\text{am}}/2$ . In this representation, the matrix form of the Hamiltonian (46) is

$$\begin{aligned} \langle 2m_a; n_m | H_{\text{am}} | 2m_a; n_m \rangle &= (\epsilon_a - n_b) g m_a (M - m_a) \\ \langle 2(m_a - 1); n_m + 1 | H_{\text{am}} | 2m_a; n_m \rangle &= \langle 2m_a; n_m | H_{\text{am}} | 2(m_a - 1); n_m + 1 \rangle \\ &= \frac{1}{2} \frac{m_a (m_a - 1) (M - n_b)}{m_a (m_a - 1) (M - n_b)}; \end{aligned}$$

Similarly, for our model the matrix form of the Hamiltonian (31) in the "pair number" representation is

$$\begin{aligned} \langle n_b; n_p | H | n_b; n_p \rangle &= (\epsilon_b - n_a) g (n_b + M + 1) (M - n_p) \\ \langle n_b - 1; n_p + 1 | H | n_b; n_p \rangle &= \langle n_p; n_b | H | n_b - 1; n_p + 1 \rangle \\ &= \frac{1}{2} \frac{n_p (n_b + M + 1) (M - n_b)}{n_b (n_b + M + 1) (M - n_b)}; \end{aligned}$$

where

$$M = \frac{N_{\text{am}}}{2}; \quad (48)$$

with  $M > 0$ . In the limit  $M \rightarrow \infty$ , that is, when we can neglect  $M \approx M - 1$  and other terms of order of  $1/M$ , these two Hamiltonians are same under the transformations  $n_a \leftrightarrow n_p$  and  $n_m \leftrightarrow n_b$ .

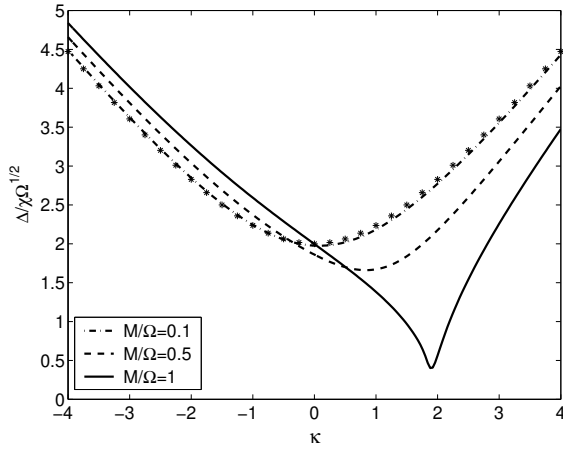


FIG. 4: Lowest excitation energies as a function of  $\kappa$  for  $M = 1$  (solid line) and  $M = 0.5$  (dashed line), and  $M = 0.1$  (dash-dotted line), at fixed pair number  $M = 120$ , where  $g = 0$ . The asterisks correspond to a linear approximation for small  $M$  (see text).

### 3. Intermediate regime

The behavior of the system apart from these two limiting cases deviates from both models. The most striking difference between these regimes appears in the energy,  $E$ , of the first excited state. Figure 4 shows  $E$  in the absence of pairing interaction for  $M = 1$  (solid line),  $M = 0.5$  (dashed line), and  $M = 0.1$  (dash-dotted line) as a function of  $\kappa$  for fixed  $M = 120$ . In the case of  $M = 0.1$ ,  $E$  agrees well with the one-particle energy difference  $E_+ - E_- = \frac{1}{2} + 4\kappa^2$  of the linear coupled-boson model (45) (shown as asterisks in the figure). Increasing  $M$  shifts the location of the minimum of the energy gap and reduces the value of its minimum. For  $M = 1$ , namely, the minimum gap approaches zero at  $\kappa = 2$ , consistently with a transition point in the atom-molecule condensate system [40, 42]. This result is indicative of the appearance of a quantum phase transition in the limit  $M \rightarrow 1$ .

### C. The role of the pairing interaction

We now examine in more detail the ground-state statistics of the molecular field in the presence of pairing interaction  $V_p$ . Since the cases of  $M = 1$  and  $M = 0.1$  can be mapped onto relatively well-known systems, we present results for the situation of a half-filled shell,  $M = 0.5$ , only. Figures 5 and 6 show the probability  $P(n_b)$  of having  $n_b$  molecules in the trap, the molecule statistics, for  $2M = 120$  as a function of the dimensionless parameter  $\kappa$ , with  $g = 0$  and  $g = 10$ , respectively. There are several quantitative differences between the two cases: the transition from an atomic to a molec-

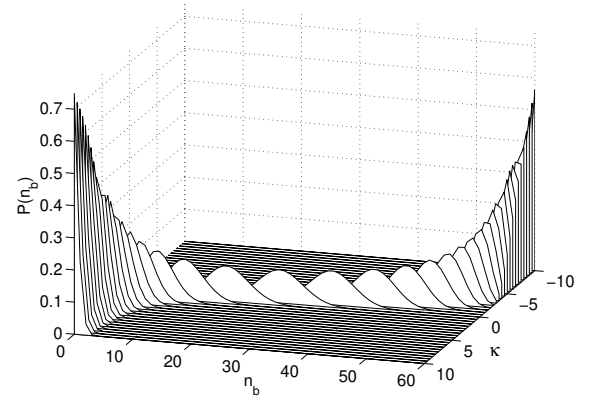


FIG. 5: Molecule statistics  $P(n_b)$  as a function of the dimensionless parameter  $\kappa$  in the absence of pairing interaction,  $g = 0$ , for  $2M = 120$ .

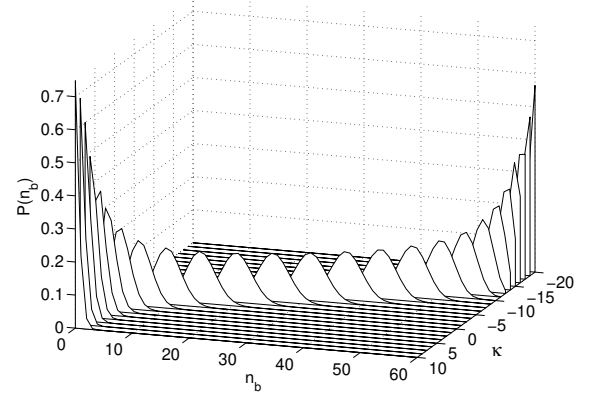


FIG. 6: Molecule statistics  $P(n_b)$  as a function of the dimensionless parameter  $\kappa$  in the presence of pairing interaction,  $g = 10$ , for  $2M = 120$ .

ular ground state is shifted by the pairing interaction, and the width of the crossover region in detuning space is significantly broader.

This behavior can be understood by noting that the pairing interaction gives rise to an additional detuning effect depending on the number of molecules, as shown by the diagonal terms of the Hamiltonian (48) with  $M = M = 2$ . This interaction leads to number-dependent energy shifts and dephasing between different molecular number states. A similar effect has been studied in the context of a Jaynes-Cummings-like description of photoassociation and has been referred as "nonlinear detuning" [44].

We can estimate the position of the "resonance" point  $\kappa_{\text{res}}(g)$  where the ground state goes from being molecular to atomic in nature by taking  $n_b = M = 2 + 1$ ;  $n_p = M = 2 - 1$   $\hbar n_b = M = 2 + 1$ ;  $n_p = M = 2 - 1$   $i = \hbar n_b = M = 2$ ;  $n_p = M = 2$   $\hbar n_b = M = 2$ ;  $n_p = M = 2$ . This gives

$$\kappa_{\text{res}}(g) = \frac{g}{2};$$



where we have neglected a term of order  $1/\eta$ .

The shift in  $|\psi_{\text{res}}\rangle$  due to the pairing interaction is further illustrated in Fig. 7, which shows the magnitude of the joint coherence function,  $|\mathcal{G}_{\text{am}}|$ , as a function of  $\kappa$  for three values of the pairing coefficient  $g$ . Finally, Fig. 8 shows the entanglement entropy  $E(\rho_b)$  of the ground state, obtained from the von Neumann entropy of the molecular reduced density operator [43]

$$\rho_b = \text{Tr}_f(\rho);$$

as

$$E(\rho_b) = -\sum_{n_b=0}^{X_M} \mathcal{P}(n_b) \log_2 \mathcal{P}(n_b); \quad (49)$$

where the logarithm is taken in base 2, for three values of the pairing interaction strengths,  $g = 0; 5; 10$ . The entanglement in Figure 8 is divided by a maximum entanglement,  $\log M$ . Consistently with the results of Figs. 5 and 6 for the molecular statistics, the pairing interaction reduces the entanglement.

#### IV. DYNAMICS

In the absence of pairing interaction our model is equivalent to the Tavis-Cummings model, whose dynamics has been studied in detail in the context of coherent spontaneous emission from a system of  $N$  two-level atoms interacting with a quantized radiation field [23, 24]. The main purpose of this section is to extend this work to the study of the system dynamics in the presence of  $V_p$ . One important result is that the nonlinearity of this interaction produces a self-trapping transition.

We assume that the system consists initially either of atomic pairs or of molecules only, corresponding to a maximal spin state. A photoassociation beam is applied from  $t = 0$  on, and we examine the subsequent coherent dynamics of the system. Note that although this problem resembles the dynamics of a bosonic Josephson Junction [27, 28] in an asymmetric trap for the initial imbalance in populations, the nonlinear coupling term in our model leads to considerably richer dynamics. Since the total spin is a constant of motion of the Hamiltonian (31), we confine our discussion to the maximal spin state  $\mathcal{S} = \pm 2i$ .

##### A. Semiclassical approximation

Before proceeding with a full quantum analysis, we first consider the semiclassical approximation. Our approach is very similar to that taken in Ref. [41]. Introducing the two operators

$$\begin{aligned} J_+ &= S^\dagger b; \\ J_- &= b^\dagger S; \end{aligned} \quad (50)$$

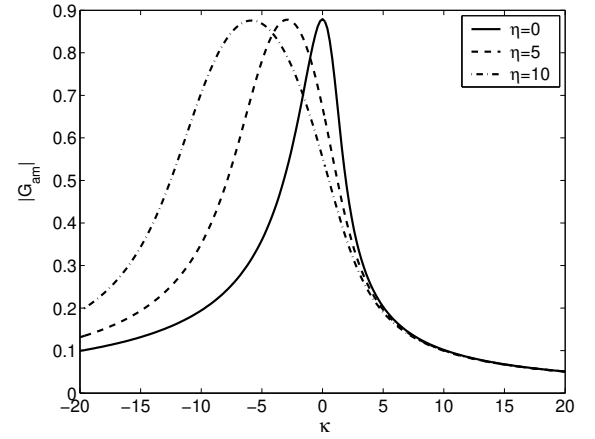


FIG. 7: Normalized joint coherence,  $|\mathcal{G}_{\text{am}}|$ , of the ground state as a function of  $\kappa$  for three values of the pairing interaction strengths  $g = 0, 5, 10$ , indicated in the insert.

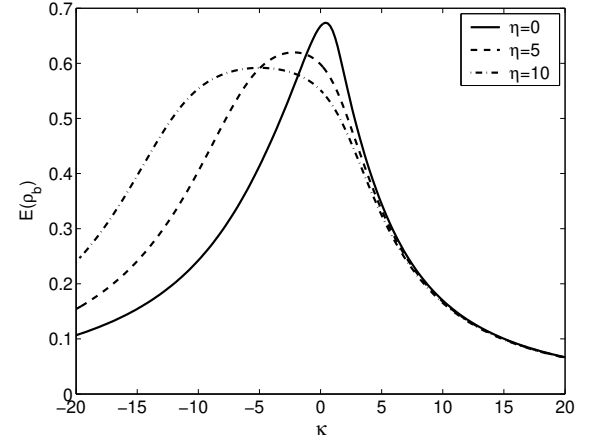


FIG. 8: Entanglement entropy,  $E(\rho_b)$ , of the ground state, in units of the maximum entanglement  $\log M$ , as a function of  $\kappa$  for three values of the pairing interaction strengths  $g = 0, 5, 10$ , indicated in the insert.

results in the Heisenberg equations of motion

$$i\frac{d}{dt}J_+ = [J_+, H] = 2b^\dagger b S^z + S^\dagger S - 2gJ_- S^z; \quad (51)$$

$$i\frac{d}{dt}J_- = [J_-, H] = -2b^\dagger b S^z - S^\dagger S + 2gS^z J_-; \quad (52)$$

$$i\frac{d}{dt}S^z = [S^z, H] = (J_+ - J_-); \quad (53)$$

Here we note the following relations between operators and conserved quantities,

$$S^\dagger S = S(S+1) - S^z(S^z+1); \quad b^\dagger b = M - S - S^z;$$

As usual we introduce a semiclassical approximation by factorizing the mean values of the various operators that appear in the Heisenberg equations of motion, such as  $\langle b^\dagger b J_+ \rangle = \langle b^\dagger b \rangle \langle J_+ \rangle$  and  $\langle J_- S^z \rangle = \langle J_- \rangle \langle S^z \rangle$ ,

etc. Introducing the c-number functions  $s_z = \hbar s_z i$ ,  $j_x = \hbar(j_x + j_x^\dagger)i/2$ , and  $j_y = \hbar(j_y - j_y^\dagger)i/2$ , and neglecting corrections of order  $1/M$ , that is, setting  $\hbar S^\dagger S = S^2 = s_z^2$ , we obtain the semiclassical equations of motion

$$\frac{d}{dt} j_x = -j_y - 2g j_y s_z \quad (54)$$

$$\frac{d}{dt} j_y = j_x + 2g j_x s_z - \hbar(s_z) \quad (55)$$

$$\frac{d}{dt} s_z = -2j_y; \quad (56)$$

where  $\hbar(s_z) = 3s_z^2 + 2(M - S)s_z + S^2$ . Noting the additional conserved quantity

$$\frac{d}{dt} j_x - \frac{1}{2}s_z + \frac{g}{2}s_z^2 = 0;$$

we find that the coupled equations (54) are equivalent to the classical Newtonian equation of motion

$$\frac{d^2}{dt^2} s_z = -\frac{d}{ds_z} U(s_z); \quad (57)$$

where the potential  $U(s_z)$  is determined by the initial conditions for  $j_x(0)$  and  $s_0 = s_z(0)$ . It is sufficient for our purpose to assume an initial Fock state, so that  $j_x(0) = 0$  and  $U(s_z)$  is given by

$$\begin{aligned} U(s_z) = & \frac{g^2}{2} s_z^4 - (g! + 2^{-2}) s_z^3 \\ & + \frac{1}{2} + g! s_0 - g^2 (s_0)^2 + 2^{-2} (M - S) s_z^2 \\ & + 2^{-2} S^2 - \frac{1}{2} s_0 + \frac{1}{2} g s_0^2 s_z; \end{aligned} \quad (58)$$

Since the potential has a quartic form of  $s_z$ , Eq. (57) can be solved analytically in terms of Jacobian elliptic functions. The derivation of the general solutions, which is straightforward but lengthy, is given in Appendix A.

## B. Coherent dynamics, $g = 0$

We first examine a typical behavior of the semiclassical dynamics in the absence of pairing interaction,  $g = 0$ , for  $M = 1$ ,  $M = 0.5$ , and  $M = \infty$ .

From the semiclassical solutions (A8) in the case of  $g = 0$  and on the exact resonance  $\omega = 0$ , the population in balance between fermionic pairs and molecules,  $\langle n_{p,i} \rangle = \langle n_{b,i} \rangle = 2S - M + 2s_z$ , and the coherence function  $j_y$  is given by

$$\frac{\langle n_{p,i} \rangle - \langle n_{b,i} \rangle}{M} = 2 \operatorname{sn}^2 \left( \sqrt{\frac{P}{t}}; k \right) - 1; \quad (59)$$

$$\begin{aligned} \frac{2j_y}{P} = & 2 \operatorname{sn} \left( \sqrt{\frac{P}{t}}; k \right) \operatorname{cn} \left( \sqrt{\frac{P}{t}}; k \right) \\ & \operatorname{dn} \left( \sqrt{\frac{P}{t}}; k \right); \end{aligned} \quad (60)$$

where  $\operatorname{sn}$ ,  $\operatorname{cn}$ , and  $\operatorname{dn}$  are Jacobian elliptic functions [45]. Here,  $k = \sqrt{M/(M+1)}$  is the elliptic modulus and  $\omega$  is a

phase factor determined by the initial conditions. It is equal to  $\omega = K$ , corresponding to the complete elliptic integral of the first kind, for an initial fermionic Fock state  $j_p = M i$ , and to  $\omega = 0$  for an initial entire population being in the molecular mode. We note that  $j_x(t)$  is zero for all time on the exact resonance.

### 1. $M = 1$ | Linear coupled-bosons regime

In this case, the elliptic modulus  $k = 1$  (see Appendix A) so that the elliptic functions in Eqs. (59) and (60) can be approximated by  $\operatorname{sn}(u; k) \approx \sin u$ ,  $\operatorname{cn}(u; k) \approx \cos u$ , and  $\operatorname{dn}(u; k) \approx 1$ , respectively. The imbalance in atomic and molecular populations which undergoes Rabi oscillations at the frequency  $2\sqrt{P}$  is given by

$$\langle n_{p,i} \rangle - \langle n_{b,i} \rangle = M \cos(2\sqrt{P}t)$$

for an initial fermionic pair state,

$$\langle n_{p,i} \rangle - \langle n_{b,i} \rangle = M \cos(2\sqrt{P}t)$$

for an initial molecular state. These results are equivalent to those obtained directly from the Hamiltonian (44). We have compared these solutions with the exact quantum mechanical dynamics obtained numerically, and checked that the linear approximation agrees with the quantum results for  $M = 1$  and for times shorter than  $t = \frac{1}{\sqrt{P}}$ .

### 2. $M = 0.5$ | Intermediate regime

Figure 9a shows the normalized population difference  $(\langle n_{p,i} \rangle - \langle n_{b,i} \rangle)/M$ , and Fig. 9b shows the normalized coherence function  $2j_y/M\sqrt{P} = 2$ , as a function of the dimensionless time  $\tau = \sqrt{P}t$  for a system initially either in a pure atomic state or a pure molecular state and for  $M = 0.5$ . The circles correspond to the semiclassical description, while the lines are the results of a full quantum-mechanical analysis. The anharmonicity due to the nonlinear atom-molecule coupling is clearly apparent, and also shows that the semiclassical dynamics approximate the quantum dynamics very well.

We note that the atomic pair state in the half-filled shell corresponds to a Dicke superradiant state [23], which is known from quantum optics to give rise to the strongest collective enhancement of transition probabilities. This enhancement is proportional to the product of the number of particle pairs  $M$  and the number of hole pairs  $M$ , and is maximum for  $M = \infty$ . From Eq. (59), we have that for sufficient short times  $t = \frac{1}{\sqrt{P}}$  the average number of molecules builds up as

$$\langle n_{b,i} \rangle = \operatorname{cn}^2 \left( \sqrt{\frac{P}{t}}; k \right)$$

$$\approx 1 - M \left( \frac{M}{M+1} \right) \left( \frac{t}{\sqrt{P}} \right)^2 = \frac{2}{4} t^2;$$

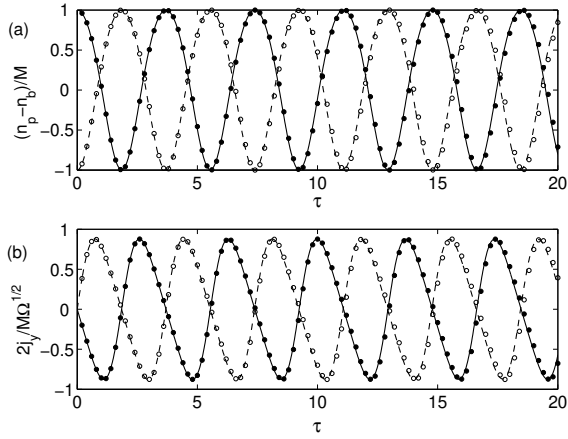


FIG. 9: Comparison of the semiclassical and quantum dynamics for  $2M = 120$ ,  $\delta = 0$ , and  $g = 0$ . Figure (a) shows the population difference between fermionic pairs and molecules  $(n_p - n_b)/M$ . Figure (b) plots the coherence function  $2j_y/M$  as a function of the dimensionless time  $\tau$ . The solid and dashed lines give the quantum results for an initial fermionic pair state and a pure molecular state, respectively. The corresponding semiclassical results are indicated by filled and open circles, respectively.

### 3. $M = 1$ | Binary atomic-molecular BEC

As shown in Ref. [26], the coherent dynamics in this regime is qualitatively very similar to that of binary condensate of atoms and molecules. For  $M = 1$ , corresponding to  $k = 1$ , the population imbalance between atomic pairs and molecules is given in the semiclassical approximation by

$$\frac{n_p - n_b}{M} = 2 \tanh^2 \left( \frac{p}{t + \frac{1}{2}} \right) - 1; \quad (61)$$

indicating that the point  $n_p = M$  is stationary. However, the system is dynamically unstable against small fluctuations, see Ref. [41] for a detailed discussion in the context of binary condensates of atoms and molecules and Ref. [46] in the context of second-harmonic generation.

### C. Self-trapping transition and quantum dynamics

To conclude, we discuss the coherent dynamics of the system in the presence of pairing interaction,  $g \neq 0$ , considering only the case of half-filling for simplicity. We consider specially the example  $2M = 120$ , which corresponds to  $n_F = 14$ , and take an initial state as the Fock state  $|j_p = M; n_b = 0\rangle$ . Figure 14 of the appendix shows the phase diagram of the semiclassical dynamics in the  $(\delta, g)$  space, illustrating that a self-trapping transition [27, 29] takes place when varying the dimensionless detuning frequency  $\delta = \omega - \omega_c$ , provided that the

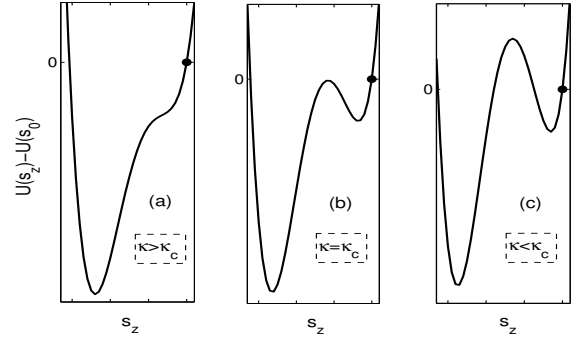


FIG. 10: Schematic potential curves,  $U(s_z) - U(s_0)$ , around a self-trapping transition point  $s_0$ . These curves are at (a) above  $s_0$ , (b) at transition point  $s = s_0$ , and (c) below  $s_0$ . The filled circle indicates an initial position of classical particle.

pairing interaction strength  $g = g^p$  exceeds a critical strength  $g_c$ . For the case of half-filling case, we find  $g_c = 5.0302$ .

This transition can be interpreted physically from the motion of "classical particle" in the "potential" (58). Figure 10 displays schematic potential curves,  $U(s_z) - U(s_0)$  as a function of  $s_z$  in the vicinity of a self-trapping transition point  $s_0$ . For our specific initial conditions the particle "velocity" is initially zero,  $ds_z(0)/dt = j_y(0) = 0$ . For  $\delta > 0$ , Fig. 10-(a), the classical particle oscillates periodically in the potential. As  $\delta$  approaches  $s_0$ , one additional potential barrier appears, and at the transition point its height equals the initial potential energy of the particle (see Fig. 10-(b)). At that point, the particle rests on the potential maximum after reaching it. Below the critical point, the barrier confines the particle in a narrow range, as shown in Fig. 10-(c). The self-trapping effect provides a sudden suppression of the amplitude of coherent oscillations. Since the key factor in achieving this transition is the quartic term in the potential (58), it disappears in the absence of pairing interaction.

Fig. 11 shows the time evolution of the population difference  $(n_p - n_b)/M$  for  $\delta = 6$  and for several detuning energies. The semiclassical solutions (dashed lines) clearly show the self-trapping as a sudden suppression of coherent oscillations from just above to just below the transition detuning. The dotted line in Fig. 11-(c) corresponds to the semiclassical solution for the threshold detuning  $\delta_0 = 3.2307$ . The solid lines show the exact quantum solutions. Apart from the transition point, the quantum and semiclassical dynamics are similar at least for short enough times. However, the oscillations of the quantum solution deviate from those of the semiclassical solution near the transition point, Fig. 11(b-c). Since in the semiclassical picture the height of the potential barrier near the transition point is just below or above the initial potential energy of a particle, the quantum motion of the particle is very sensitive to fluctuations and hence deviates significantly from its classical counterpart.

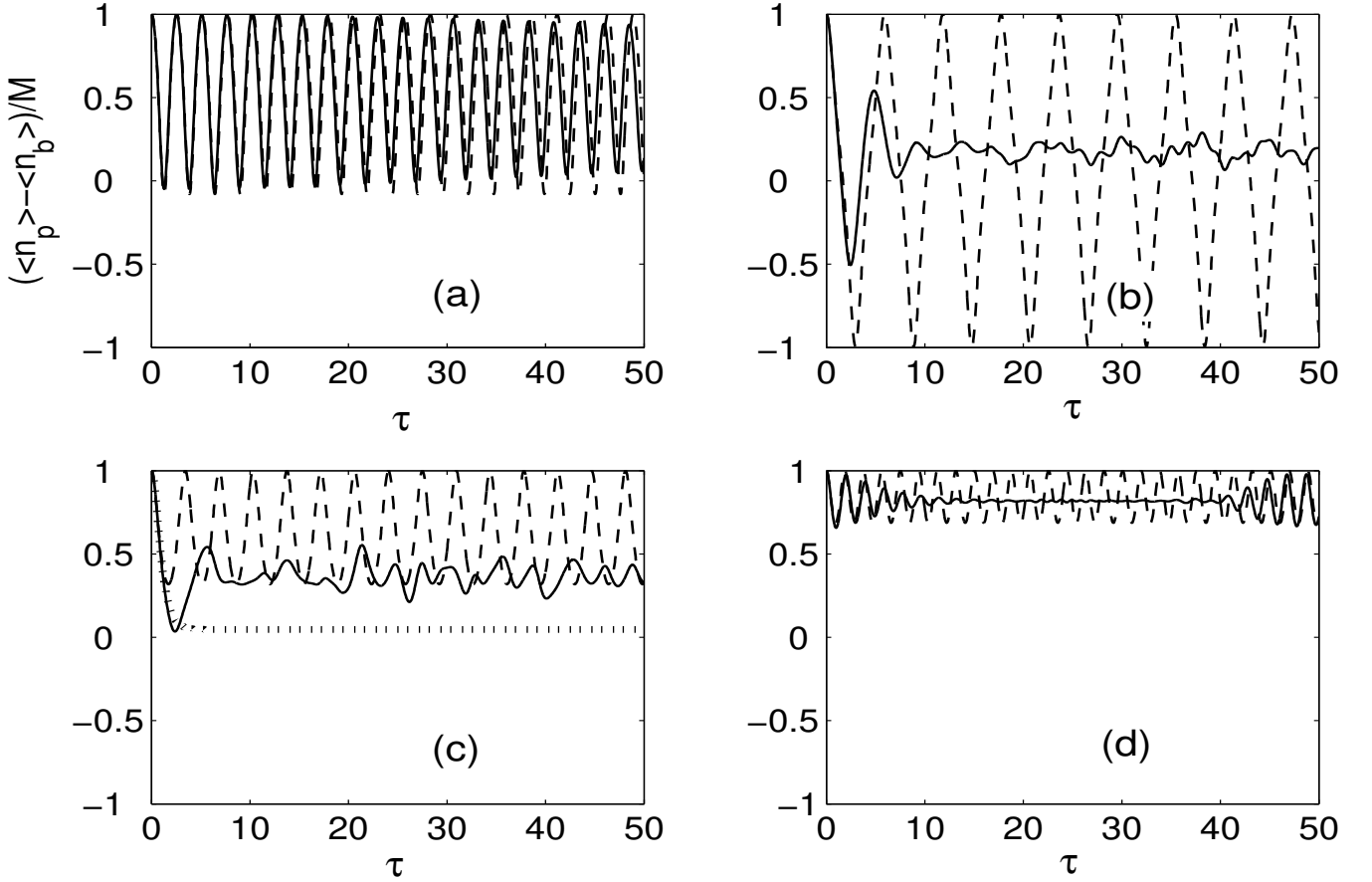


FIG. 11: Population in balance versus the rescaled time  $\tau = \frac{p}{\hbar} t$  for  $\hbar = 6$ . Quantum (solid line) and semiclassical (dashed line) solutions are shown, respectively, for the detuning parameters (a)  $\Delta = 0$  and (b)  $\Delta = 3.1$ , and (c)  $\Delta = 3.3$ , and (d)  $\Delta = 4.0$ . The dotted line in (c) corresponds to the semiclassical solution at the transition point  $\omega_0 = 3.2307$ .

The initial Fock state provides fluctuations of coherence, and large quantum fluctuations of the population in balance arise as a result. We have verified numerically that the number fluctuations near the transition point are enhanced by an order of magnitudes as compared to those far away from that point.

Figs. 12 and 13 compare the quantum and semiclassical time-averaged population in balance as a function of  $\Delta$  for  $\hbar = 2.0$ , and for  $\hbar = 6.0$ , respectively. In contrast to the second case, there is no self-trapping transition in the first case. Hence the semiclassical time-averaged population in balance (cross) is a smooth function of  $\Delta$ , and agrees well with the quantum results. For the strong pairing coupling of Fig. 13, in contrast, an abrupt jump of the semiclassical time-averaged value occurs when varying  $\Delta$ , a signature of the self-trapping transition. Due to the large quantum fluctuations, it differs markedly from the time-averaged quantum result near a transition point.

## V. SUMMARY

In this paper, we have considered the coherent photoassociation of fermionic atoms into bosonic molecules trapped in a spherically symmetric harmonic trap. We showed that under a realistic set of conditions this system can be mapped onto a Tavis-Cummings Hamiltonian with an additional pairing interaction using pseudo-spin operators. We carried out an exact numerical diagonalization of the Hamiltonian to determine the ground state of the system, investigating the crossover from a predominantly atomic to a predominantly molecular state. We also investigated the joint coherence and the quantum entanglement between the atomic and molecular fields, and found that the atomic pairing interaction suppresses the entanglement between fermions and bosons. We then analyzed the coherent dynamics of photoassociation due to the nonlinear atom-molecule coupling. Using a semiclassical factorization ansatz, we showed the appearance of a self-trapping transition in the presence of pairing interaction. An exact quantum solution illustrated the impor-

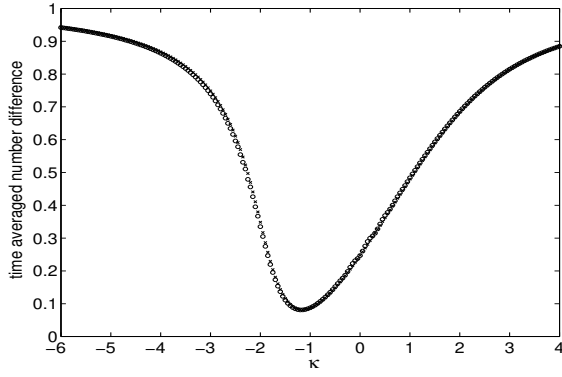


FIG. 12: Time-averaged population in balance as a function of  $\kappa$  for  $g = 2.0$ . Quantum result (cross) and semi-classical result (open circle).

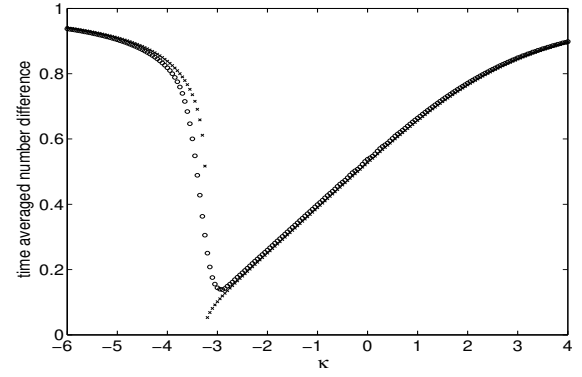


FIG. 13: Time-averaged population in balance as a function of  $\kappa$  for  $g = 6.0$ . Quantum result (cross) and semi-classical result (open circle).

tant role of quantum fluctuations in the neighborhood of that transition point. Future work will extend this study to a detailed analysis of the non-degenerate model and to multiwell superradiant systems. For instance, preparing an atomic Fermi gas in a Josephson-type configuration and applying a photoassociation beam should lead to the efficient production of spatially correlated molecules.

#### Acknowledgments

This work is supported in part by the US Office of Naval Research, the National Science Foundation, the US Army Research Office, NASA, and the Joint Services Optics Program.

#### APPENDIX A: ANALYTIC SOLUTIONS IN TERMS OF JACOBIAN ELLIPTIC FUNCTIONS

In this appendix, we obtain analytic solutions of semi-classical dynamics that obey the Newtonian equation of motion Eq. (57), and show the phase diagram of the semi-classical dynamics based on those solutions.

The solution of Eq. (57) has the general form

$$t = \int_{s_0}^{s_z} \frac{ds}{\sqrt{2[U(s_0) - U(s)]}}; \quad (\text{A1})$$

with the potential  $U(s_z)$  given by Eq. (58).

We analyze the solution for the two cases  $g = 0$  and  $g \neq 0$ , separately, and for simplicity we take the initial

state as an atomic state in the maximum spin manifold  $S = \pm 2$ . The extension to other initial states is straightforward.

##### 1. Case $g = 0$

In this case, the "potential"  $U(s_z)$  is a cubic function of  $s_z$ ,

$$U(s_z) = -\frac{1}{2} s_z^3 + \frac{1}{2} s_0^2 s_z^2 + \frac{1}{2} S^2 - \frac{1}{2} s_0 s_z; \quad (\text{A2})$$

Here we have used the initial condition  $s_0 = S + M$ . By introducing the normalized quantities

$$s_z = s_z / 2S \quad (-1/2 \leq s_z \leq 1/2); \quad s_0 = s_0 / 2S;$$

we obtain the explicit form of the denominator of the right-hand side of Eq. (A1),

$$\begin{aligned} r(s_z) &= 2[U(s_0) - U(s_z)] \\ &= 4S^2(2S)^3(s_z - s_0)(s_z - s_+)(s_z - s_-) \quad (\text{A3}) \\ s &= \frac{1}{8} \sqrt{\frac{1}{16s_0^2 + 16}}; \quad (\text{A4}) \end{aligned}$$

where  $s_{\pm} = \pm \frac{1}{2} - \frac{s_0}{2S}$ . We note that the variables  $s$  are always real-valued for any magnitudes of  $s_0^2$ , because  $-1/2 \leq s_0 \leq 1/2$ , and then  $s_+ \geq s_0 \geq s_-$ . The solution can be obtained by integrating the form

$$t = \int_{s_0}^{s_z} \frac{ds}{r(s_z)} = -\frac{1}{2S(s_+ - s_-)} \int_0^{\frac{1}{2} \sqrt{\frac{1}{16s_0^2 + 16}}} \frac{d}{k^2 \sin^2}; \quad (\text{A5})$$

where,

$$s(t) = \arcsin \frac{s_+ - s_-}{(s_0 - s_-)(s_+ - s_-)}; \quad (A 6)$$

The integral that appears in that equation is an elliptic integral of the first kind. Noting that the integration within  $0 \leq t \leq 2\pi$  gives rise to a complete elliptic integral of the first kind,  $K$ , we find

$$P \frac{1}{2S(s_+ - s_-)} t + K = \text{sn}^{-1}(\sin(t); k) \quad (A 6)$$

where the function  $\text{sn}^{-1}$  is the inverse of the Jacobian elliptic function and  $k = \frac{s_+ - s_-}{(s_0 - s_-)(s_+ - s_-)}$  denotes the elliptic modulus. This gives the evolution of  $s_z(t)$

$$s_z(t) = s_- + (s_0 - s_-) \text{sn}^2 \left( P \frac{1}{2S(s_+ - s_-)} t + K; k \right) \quad (A 7)$$

At the exact resonance  $\Delta = 0$ , we have that  $s_+ = 1/2$ ,  $s_- = -1/2$ , and  $k = \frac{1}{M} = 2S$  so that this expression reduces to

$$s_z(t) = S + M \text{sn}^2 \left( P \frac{1}{2St} + K; k \right) \quad (A 8)$$

In terms of  $s_z(t)$  the coherence functions  $j_x(t)$  and  $j_y(t)$  are given by

$$j_x(t) = \frac{1}{2} s_z(t); \quad j_y(t) = \frac{1}{2} \frac{ds_z(t)}{dt} \quad (A 9)$$

This results in the expressions for the difference in atomic and molecular populations  $n_{p,i} - n_{b,i}$ , and the coherence function  $j_y$  of Eqs. (59) and (60), respectively.

## 2. Case $g \neq 0$

The presence of pairing interaction renders the potential quartic in  $s_z$ , see Eq. (58) where we have again as-

sumed that the initial state is an atomic state of maximum spin,  $\mathcal{S}; S + M$ . It is convenient to introduce the function  $f(s_z)$  as

$$f(s_z) = g^2 (2S)^4 (s_z - s_0) f_4(s_z); \quad (A 10)$$

where

$$f(s_z) = s_z^3 + s_z^2 + s_z + (s_z - s_1)(s_z - s_2)(s_z - s_3); \quad (A 11)$$

$$= s_0 - 2 = -4 = -2, \quad s_1 = \frac{2}{3} + \frac{2}{3} = \frac{4}{3}, \text{ and } s_2 = \frac{2}{3} + \frac{2}{3} = \frac{4}{3}$$

$$2s_0^2 = -2s_0^2 + 1 = -1 \text{ with } s_3 = \frac{2}{3} = \frac{2}{3}.$$

The variables  $s_1, s_2$ , and  $s_3$ , which correspond to the roots of the cubic equation,  $f(s_j) = 0$ , are obtained by "Cardano's formula". With  $\Delta = 3$ ,  $p = -2/3$ , and  $q = 2/3 = 2/3$ , and also  $D = (4p^3 + 27q^2)$ , those roots are given by

$$s_j = \frac{1}{3} + \omega^j \sqrt[3]{\frac{q}{2} + \frac{1}{6} \sqrt{D}} + \omega^{j+1} \sqrt[3]{\frac{q}{2} - \frac{1}{6} \sqrt{D}}; \quad (A 12)$$

where  $j = 1; 2; 3$ .

The numbers of real and complex roots are determined by the sign of the polynomial discriminant  $D$ . If (a)  $D > 0$ , all three roots are real and unequal. If (b)  $D < 0$ , one root is real and two are complex conjugates. If (c)  $D = 0$ , two roots are equal for  $q \neq 0$ , and all roots are equal for  $q = p = 0$ .

### a. Case $D > 0$

Suppose that  $s_0 < s_1 < s_2$ , and  $s_a > s_b > s_c$  or  $s_b > s_c > s_0$ , where each  $s_{a,b,c}$  corresponds to one of the roots  $s_j$ 's. The solution of Eq. (A 1) reads then

$$t = \int_{s_0}^{s_z} \frac{ds}{f(s)} = \frac{1}{gS} \int_{s_0}^{s_z} \frac{d}{(s_0 - s_1)(s_a - s_2)} \frac{1}{1 - k^2 \sin^2}; \quad (A 13)$$

where

$$s(t) = \arcsin \frac{(s_a - s_1)(s_0 - s_2)}{(s_0 - s_1)(s_a - s_2)}; \quad k = \frac{(s_0 - s_1)(s_b - s_2)}{(s_0 - s_1)(s_a - s_2)}; \quad (A 14)$$

so that

$$s_z(t) = \frac{s_0(s_a - s_1) + s_c(s_0 - s_1) \text{sn}^2}{(s_a - s_1) + (s_0 - s_1) \text{sn}^2} \frac{P \frac{1}{gS} \frac{1}{(s_0 - s_1)(s_a - s_2)} t; k}{P \frac{1}{gS} \frac{1}{(s_0 - s_1)(s_a - s_2)} t; k}; \quad (A 15)$$

### b. Case $D < 0$

Letting  $s_a$  label the real root and with  $s_b = s_c = s_R + is_I$ , we have that  $f(s_z) = g^2 (2S)^4 (s_z - s_0) (s_z - s_R)^2 + s_I^2$ . With the change of variable from

$s_a - (s_z - s_R)^2 + s_I^2$ . With the change of variable from

$s_z(s_0, s_a, s_b)$  to

$$\frac{s_0 - s_a}{s_z - s_a} = \frac{A}{B} \frac{1 - \cos \phi}{1 + \cos \phi}; \quad (\text{A } 16)$$

where  $A = \frac{p}{(s_0 - s_a)^2 + s_I^2} > 0$  and  $B = \frac{p}{(s_a - s_b)^2 + s_I^2} > 0$ , and taking the elliptic modulus

as

$$k = \frac{r}{4AB} \frac{(s_0 - s_a)^2 (A - B)}{A + B}; \quad (\text{A } 17)$$

the integral Eq. (A 1) can then be replaced by

$$t = \int_{s_0}^{s_z} \frac{ds}{\sqrt{f(s)}} = \frac{1}{2gS} \int_0^{\phi} \frac{d\phi}{1 - k^2 \sin^2 \phi}; \quad (\text{A } 18)$$

The semiclassical solution is then given by

$$s_z(t) = \frac{s_a A + s_0 B - (s_a A - s_0 B) \text{cn} \left( \frac{2gS}{AB} t; k \right)}{A + B - (A - B) \text{cn} \left( \frac{2gS}{AB} t; k \right)}; \quad (\text{A } 19)$$

c. Case  $D = 0$

In this case, the solution of Eq. (A 1) can be expressed in terms of elementary functions. For  $q \neq 0$  the solutions are equivalent to Eq. (A 15) in which the elliptic functions are replaced by trigonometric functions for  $k = 0$  ( $s_b = s_c$ ), or hyperbolic functions for  $k = 1$  ( $s_0 > s_a = s_b$ ). If  $q = p = 0$ , the function  $f(s_z)$  has triple degenerate roots at a point  $s_a = s_b = s_c$ , and the corresponding solution is obtained by

$$s_z(t) = s_a + \frac{s_0 - s_a}{1 - f - gS(s - s_a) \tanh^2}; \quad (\text{A } 20)$$

### 3. Phase diagram of semiclassical dynamics

In this subsection, we discuss the structure of the semiclassical dynamics in parameter space for the specific case of a half-filled shell,  $2M = 1$ , by calculating the elliptic modulus of the semiclassical solution.

For  $g = 0$ , Eq. (A 7) describe all possible dynamics for arbitrary detuning energy  $\epsilon$ , while in the presence of a pairing interaction the dynamics is given by solutions (A 15) and (A 19), depending on the sign of  $D$ . The dynamics is described by Eq. (A 20) at a single singular point in parameter space, as we shall see later.

Figure 14 shows the elliptic modulus of the semiclassical solution in parameter space. The two regions  $D > 0$  and  $D < 0$  are separated by  $D = 0$  lines that correspond to the specific values of elliptic modulus  $k = 0$  and  $k = 1$ . Eqs. (A 15) and (A 19) coincide for  $k = 0$ , which corresponds to the white lines in Fig. 14. Hence these two solutions connect continuously when crossing that line. For the black line  $k = 1$ , on the other hand, solutions

corresponding to Eq. (A 15) differ from Eq. (A 19). This

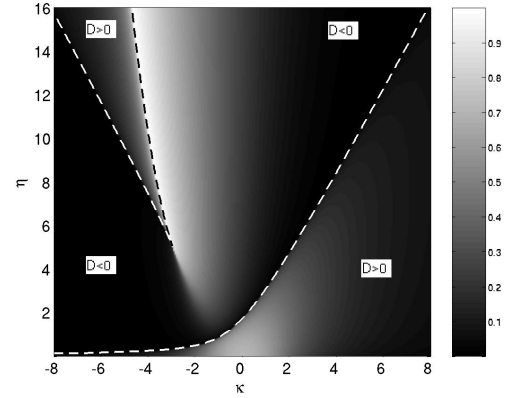


FIG. 14: Elliptic modulus in parameter space for the half-filled shell:  $2M = 1$ .

discontinuity gives rise to the self-trapping transition discussed in subsection IV C.

Figure 14 shows that the black line and one of the white lines intersect at the critical point  $(\epsilon_c; \kappa_c)$ , where  $q = p = 0$ , given explicitly by

$$\epsilon_c = 2 \frac{r}{3} (45 + 26 \frac{p}{3})^{1/4}, \quad 5.0302 \quad (\text{A } 21)$$

$$\kappa_c = \frac{4}{3} (2 + \frac{p}{3}), \quad 2.9677; \quad (\text{A } 22)$$

From this result, we conclude that the self-trapping transition appears by varying the detuning parameter  $\epsilon$  only for  $\epsilon > \epsilon_c$ .

- 
- [1] R. Wynar et al., *Science* 287, 1016 (2000).
- [2] S. Inouye et al., *Nature (London)* 392, 151 (1998).
- [3] V. A. Yurovsky, A. Ben-Reuven, P. S. Julienne, and C. J. Williams, *Phys. Rev. A* 60, R765 (1999).
- [4] E. A. Donley, N. R. Claussen, S. T. Thompson, and C. E. Wieman, *Nature (London)* 417, 529 (2002).
- [5] S. Durr, T. Volz, A. Marte, and G. Rempe, *Phys. Rev. Lett.* 92, 020406 (2004).
- [6] K. Xu, T. Mukaiyama, et al., *Phys. Rev. Lett.* 91, 210402 (2003).
- [7] D. S. Petrov, C. Salomon, and G. V. Shlyapnikov, *Phys. Rev. Lett.* 93, 090404 (2004).
- [8] M. Greiner, C. A. Regal, and D. S. Jin, *Nature (London)* 426, 537 (2003).
- [9] M. W. Zwierlein et al., *Phys. Rev. Lett.* 91, 250401 (2003).
- [10] S. Jochim et al., *Science* 301, 2101 (2003).
- [11] C. A. Stan et al., *cond-mat/0406129*.
- [12] S. Inouye et al., *cond-mat/0406208*.
- [13] A. J. Kerman, J. M. Sage, S. Sainis, T. Bergeman, and D. DeMille, *Phys. Rev. Lett.* 92, 033004 (2004).
- [14] C. A. Regal, M. Greiner, and D. S. Jin, *Phys. Rev. Lett.* 92, 040403; M. Bartenstein et al., *Phys. Rev. Lett.* 92, 120401 (2004); M. Zwierlein et al., *Phys. Rev. Lett.* 92, 120403 (2004).
- [15] E. Timmermans, K. Furuya, P. W. Milonni, and A. K. Kerman, *Phys. Lett. A* 285, 288 (2001).
- [16] M. Holland, S. J. J. M. F. Kokkeimans, M. L. Chiofalo, and R. W. Alsler, *Phys. Rev. Lett.* 87, 120406 (2001); Y. Ohashi and A. Griffin, *Phys. Rev. Lett.* 89, 130402 (2002).
- [17] A. Bohr and B. R. Motelson, "Nuclear Structure" (Benjamin, New York, 1975), Vols. I and II.
- [18] C. T. Black, D. C. Ralph, and M. Tinkham, *Phys. Rev. Lett.* 76, 688 (1996).
- [19] P. W. Anderson, *Phys. Rev.*, 112, 1900 (1958).
- [20] A. Kerman, *Ann. Phys. (N.Y.)*, 12, 300 (1961).
- [21] M. Tavis and F. W. Cummings, *Phys. Rev.* 170, 379 (1968).
- [22] N. M. Bogoliubov, R. K. Bulbough, and J. Timonen, *J. Phys. A* 29, 6305 (1996).
- [23] R. H. Dicke, *Phys. Rev.* 93, 99 (1954).
- [24] R. Bonifatio and G. Preparata, *Phys. Rev. A* 2, 336 (1970).
- [25] J. Javanainen et al., *Phys. Rev. Lett.* 92, 200402 (2004); A. V. Andreev, V. Gurarie, and L. Radzihovsky, *Phys. Rev. Lett.* 93, 130402 (2004); R. A. Barankov and L. S. Levitov, *Phys. Rev. Lett.* 93, 130403 (2004).
- [26] I. Tikhonov and A. Vardi, *cond-mat/0407424*.
- [27] G. J. Milburn, J. Comey, E. M. Wright, and D. F. Walls, *Phys. Rev. A* 55, 4318 (1997); A. Smerzi, S. Fantoni, S. Giovanazzi, and S. R. Shenoy, *Phys. Rev. Lett.* 79, 4950 (1997).
- [28] J. Javanainen and M. Y. Ivanov, *Phys. Rev. A* 60, 2351 (1999); A. J. Leggett, *Rev. Mod. Phys.* 73, 307 (2001); J. R. Anglin and A. Vardi, *Phys. Rev. A* 64, 013605 (2001).
- [29] J. C. Eilbeck, P. S. Lomdahl, and A. C. Scott, *Physica D* 16, 318 (1985); A. C. Scott and J. C. Eilbeck, *Phys. Lett. A* 119, 60 (1986).
- [30] G. Racah, *Phys. Rev.* 63, 367 (1943).
- [31] see e.g. C. Cohen-Tannoudji, B. Diu and F. Laloe, "Quantum Mechanics", Vol. I Complement B<sub>VII</sub> (A Wiley-Interscience Publication, 1977).
- [32] H. Heiselberg and B. Motelson, *Phys. Rev. Lett.* 88, 190401 (2002); G. M. Bruun and H. Heiselberg, *Phys. Rev. A* 65, 053407 (2002); H. Heiselberg, *Phys. Rev. A* 68, 053616 (2003).
- [33] D. J. Heinzen, R. Wynar, P. D. Drummond, and K. V. Khentsov, *Phys. Rev. Lett.* 84, 5029 (2000).
- [34] R. W. Richardson, *Phys. Lett.* 3, 277 (1963); R. W. Richardson and N. Sherman, *Nucl. Phys.* 52, 221 (1964); R. W. Richardson, *J. Math. Phys. (N.Y.)* 6, 1034 (1965).
- [35] J. Dukelsky, C. E. S. S. Bag, and P. Schuck, *Phys. Rev. Lett.* 87, 066403 (2001).
- [36] J. Dukelsky, G. G. Dussel, C. E. S. S. Bag, and S. Pittel, *Phys. Rev. Lett.* 93, 050403 (2004).
- [37] P. Ring and P. Schuck, "The Nuclear Many-Body Problem" (Springer-Verlag, New York, 1980).
- [38] A. L. Fetter and J. D. Walecka, "Quantum Theory of Many-Particle Systems" (Dover, Mineola, NY, 2003).
- [39] T. Holstein and Primako, *Phys. Rev.* 58, 1098 (1940).
- [40] J. Javanainen and M. Mackie, *Phys. Rev. A* 59, R3186 (1999).
- [41] A. Vardi, V. A. Yurovsky, and J. R. Anglin, *Phys. Rev. A* 64, 063611 (2001).
- [42] H. Q. Zhou, J. Links, and R. H. McKenzie, *cond-mat/0207540*.
- [43] A. P. Hines, R. H. McKenzie, and G. J. Milburn, *Phys. Rev. A* 67, 013609 (2003).
- [44] C. P. Search, W. Zhang, and P. M. Eystre, *Phys. Rev. Lett.* 91, 190401 (2003); C. P. Search, T. Miyakawa, and P. M. Eystre, *Optics Express* 12, 3318 (2004).
- [45] H. Hancock: *Elliptic Integrals* (Dover Publications, Inc., New York, 1917); *Handbook of Mathematical Functions* Edited by M. Abramowitz and I. A. Stegun (Dover Publications, Inc., New York, 1972).
- [46] D. F. Walls, *Phys. Lett.* 32A, 476, (1970); D. F. Walls and C. T. Tindle, *J. Phys. A* 5, 534 (1972).